

Strong Stacking between F···H–N Hydrogen-Bonded Foldamers and Fullerenes: Formation of Supramolecular Nano Networks

Chuang Li,^[a] Yuan-Yuan Zhu,^[a] Hui-Ping Yi,^[a] Chang-Zhi Li,^[a] Xi-Kui Jiang,^[a] Zhan-Ting Li,^{*[a]} and Yi-Hua Yu^{*[b]}

Abstract: The stacking interactions between F···H–N hydrogen-bonded foldamers **1–3**, bis-foldamer **4**, and tris-foldamer **5** and C₆₀ and C₇₀ are described. Compound **4** contains two folded units, which are connected by an isophthalamide linker, whereas **5** has a C₃-symmetrical discotic structure, in which three folded units are connected by a benzene-1,3,5-tricarboxamide unit. UV/Vis, fluorescence, and NMR experiments have revealed that the foldamers or folded units strongly stack with fullerenes in chloroform.

The (apparent) association constants of the respective complexes have been determined by a fluorescence titration method. The strong association is tentatively attributed to intermolecular cooperative fluorophenyl···π and solvophobic interactions. A similar but weaker interaction has also been observed between an MeO···H–N hydro-

Keywords: fluorine • foldamers • fullerenes • hydrogen bonds • nanostructures • stacking interactions

gen-bonded foldamer and fullerenes. AFM studies have revealed that the surfaces of **3** and **4** show fibrous networks, while the surface of **5** shows particles. In sharp contrast, mixtures of **3** and **4** with C₆₀ have been shown to generate thinner separated fibrils, whereas a mixture of **5** and C₆₀ produces honeycomb-like nano networks, for which a columnar cooperative stacking pattern is proposed. The results demonstrate the usefulness of F···H–N hydrogen-bonded folded structures in the construction of nanoscaled materials.

Introduction

In recent years, there has been intense interest in the design and construction of well-defined nano architectures.^[1,2] One of the most powerful approaches is the use of reversible noncovalent interactions, such as hydrogen bonding,^[3] metal-ligand interactions,^[4] aromatic stacking, and hydrophobic interactions.^[5] Based on complementary molecular affinities, rationally designed molecular components can be

held together to produce large and elaborate architectures of high order. Fullerenes and their derivatives represent an intriguing class of spherical molecules that have many interesting photophysical, photochemical, and/or electrochemical properties.^[6] In recent years, fullerene-based nanoparticles and fullerene-pendant polymers have been extensively investigated as discrete materials.^[7,8] Nevertheless, examples of supramolecular polymeric architectures with “naked” fullerenes as assembling components are relatively limited.^[9]

In the past decade, the development of synthetic receptors for fullerenes has been mainly based on their curved π-conjugated features. Macrocyclic structures with concave cavities, such as calixarenes, cyclotriveratrylenes, cyclophanes, and cyclodextrins, represent the major family of fullerene receptors.^[10] Other types of receptors have also been reported, which among others include planar extended conjugated systems, such as porphyrins and phthalocyanines,^[11] a shape-persistent aryleneacetylene-derived macrocycle,^[12] and electron-rich TTFs.^[13] Because many of the interactions are relatively weak, ditopic receptors with two cooperative interacting units are usually used to achieve high binding stability.

Unnatural oligomers that are induced to adopt well-defined secondary structures by noncovalent interactions are known as foldamers.^[14,15] Since the first report of secondary

[a] C. Li, Y.-Y. Zhu, H.-P. Yi, C.-Z. Li, Prof. Dr. X.-K. Jiang, Prof. Dr. Z.-T. Li
State Key Laboratory of Bio-Organic and Natural Products Chemistry
Shanghai Institute of Organic Chemistry
Chinese Academy of Sciences
354 Fenglin Lu, Shanghai 200032 (China)
Fax: (+86)21-6416 6128
E-mail: ztli@mail.sicc.ac.cn

[b] Prof. Y.-H. Yu
Key Laboratory of Optical and Magnetic Resonance Spectroscopy
Ministry of Education, East China Normal University
Shanghai 200062 (China)
E-mail: yhyu@phy.ecnu.edu.cn

 Supporting information for this article is available on the WWW under <http://www.chemistry.org> or from the author.

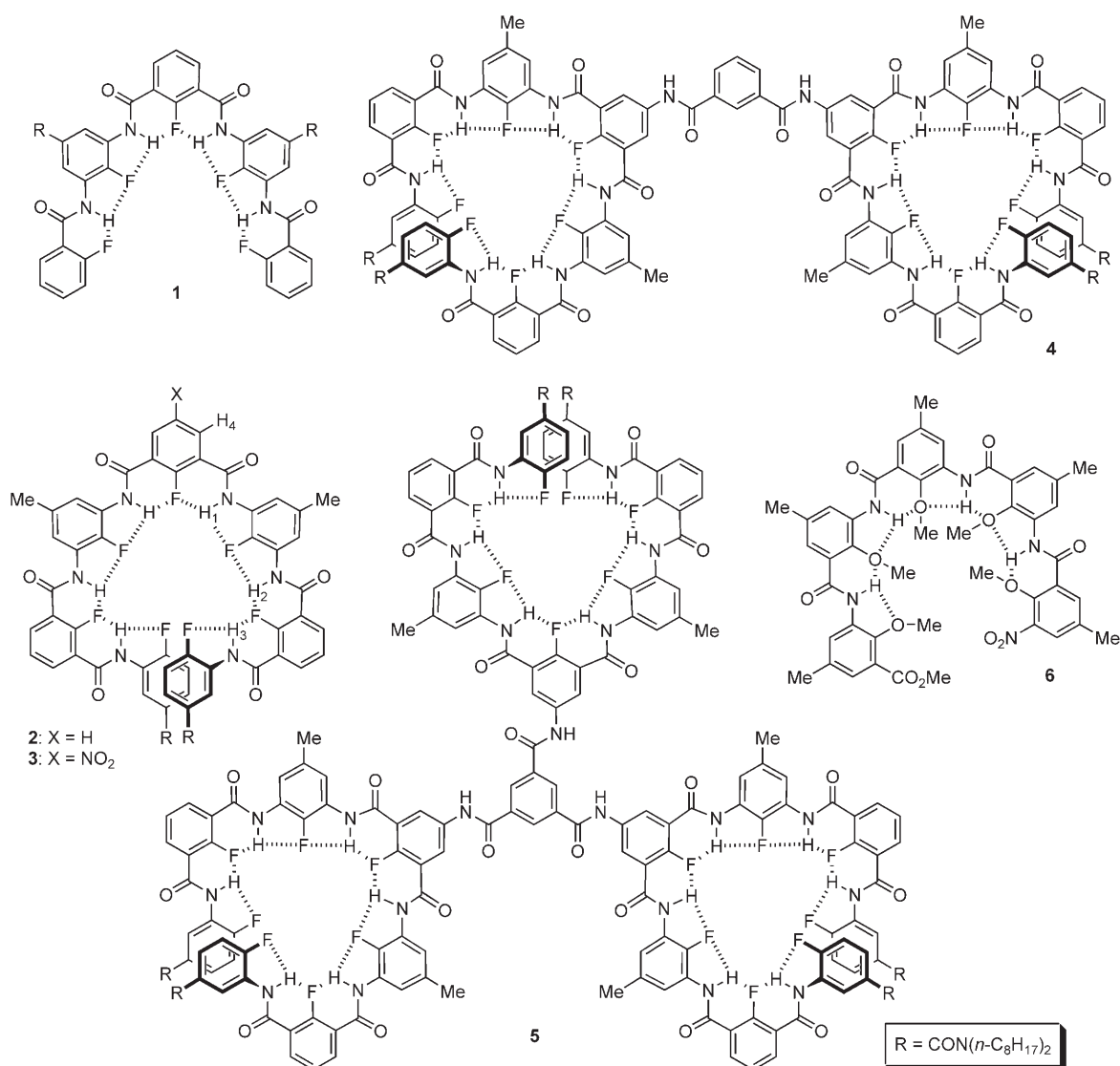
structures of anthranilamide oligomers,^[16] hydrogen-bonding-induced foldamers based on aromatic oligoamide backbones have received considerable attention, due in part to their relatively higher structural predictability.^[15,17] We have recently demonstrated that rationally designed hydrogen-bonded foldamers from aromatic oligoamides represent versatile self-assembling scaffolds^[18] and acyclic receptors for the recognition of discrete guests.^[19] Herein, we describe that 1) strong interactions are generated between F···H–N hydrogen-bonding-induced foldamers and fullerenes (C_{60} and C_{70}), and 2) that these interactions may be utilized for the construction of structurally unique supramolecular nano-networks.

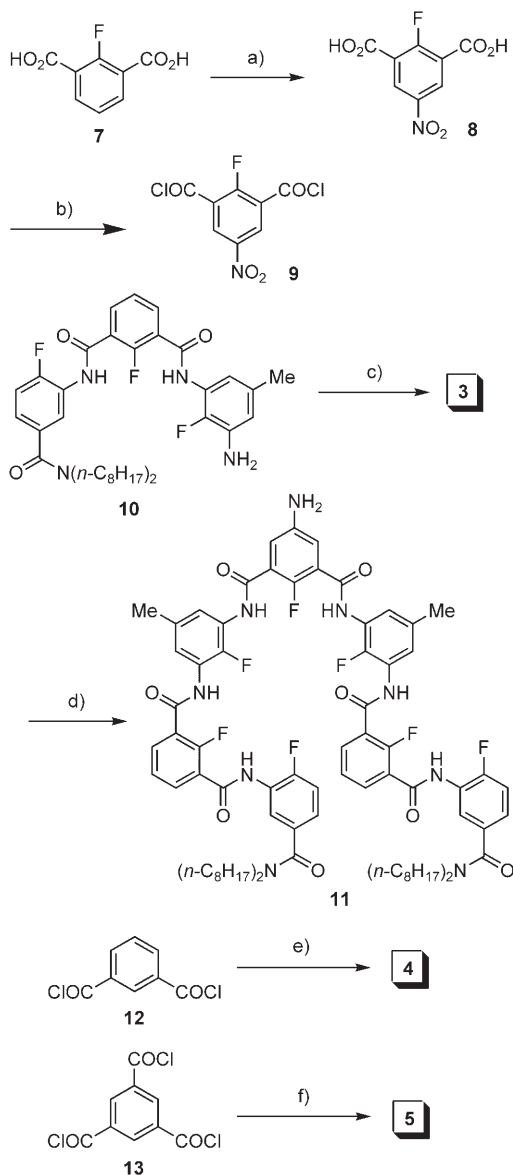
Results and Discussion

We have previously established the intramolecular five- and six-membered F···H–N hydrogen-bonding motif and have

utilized it to induce oligomers **1** and **2** to adopt folded or helical conformations.^[20] In contrast to the MeO···H–N hydrogen-bonding-driven folded analogues,^[21] in which the centrally located methyl groups are forced by the steric hindrance and angular requirements of the ether bonds to deviate from their rigidified backbones, the F···H–N hydrogen-bonded foldamers possess extended skeletons, which are reminiscent of conjugated porphyrins^[10] or rigidified planar cyclophanes.^[11] We have therefore synthesized a further three folded molecules, **3–5**, and have investigated their potential interactions with fullerenes.^[22] For comparison, the corresponding interactions of the MeO···H–N hydrogen-bonded foldamer **6**^[19d] have also been studied.

The synthetic routes to compounds **3–5** are shown in Scheme 1. Thus, diacid **7**^[20a] was first nitrated in hot oleum to give **8** in 50% yield. The nitro derivative was then treated with oxalyl chloride in THF to afford **9**, which was treated with **10**^[20b] in THF to produce foldamer **3** in 78% yield. Pd-catalyzed hydrogenation of **3** in THF gave **11** in 95% yield.





Scheme 1. Reagents and conditions: a) $\text{HNO}_3/\text{H}_2\text{SO}_4/\text{SO}_3$, 100°C , 6 h, 50%; b) $(\text{COCl})_2$, DMF (cat.), RT , 30 min; c) 9, NEt_3 , THF , RT , 2 h, 78%; d) H_2 , Pd/C (10%), THF , RT , 24 h, 95%; e) 11, NEt_3 , THF , RT , 8 h, 75%; f) 11, NEt_3 , THF , RT , 8 h, 50%.

Reactions of this amine with 12 and 13 in THF then afforded 4 and 5, respectively. Compounds 3–5 are soluble in common solvents such as toluene, dichloromethane, and chloroform, and have been characterized by ^1H NMR, ^{13}C NMR, and IR spectroscopy and by MALDI-TOF mass spectrometry.

The nitro group in 3 and the centrally located amide linkers in 4 and 5 are all distant from the groups that are involved in the intramolecular hydrogen bonding. Therefore, it is reasonable to assume that compact conformations are also formed for 3–5. Similar to that of foldamer 2, the ^1H NMR spectrum of 3 in CDCl_3 was well-resolved. Each of its amide signals appeared in the downfield region (see the Supporting Information), clearly indicating the existence of

intramolecular $\text{F}\cdots\text{H}-\text{N}$ hydrogen bonding. The resolution of the ^1H NMR spectra of 4 and 5 in CDCl_3 was very low, which may be attributed to the existence of helical isomers of their folded moieties that slowly interconvert on the ^1H NMR time scale. Although it has been reported that many fluoroaromatic molecules show a great tendency for aggregation in common organic solvents,^[23] dilution of solutions of the simple foldamers 1–3 in CDCl_3 from 3.0 mM to 0.2 mM did not cause any significant shift in the signals of their aromatic and amide protons (<0.04 ppm). Due to low resolution, similar dilution experiments could not be carried out for compounds 4 and 5. Nevertheless, within the concentration range of <0.2 mM, their UV/Vis absorbances in chloroform obeyed Beer's law (see the Supporting Information), indicating that, at least within the lower concentration range, there is no significant intermolecular aggregation for either molecule.

Mixing 1–5 with C_{60} in toluene led to a significant decrease in the absorption bands of the fullerene and an increase in the absorption bands of the oligomers in the UV/Vis spectra. Figure 1 shows some representative results. A new absorption band at around 332 nm was produced for each of the oligomers upon the addition of C_{60} . Moreover, adding the oligomers to a solution of C_{60} in toluene also caused the color of the fullerene to change from characteristic red-purple to dark brown (see the Supporting Information). All of these observations are indicative of strong complexation between the folded oligomers and C_{60} . A similar color change was also observed for C_{70} upon mixing with the oligomers in toluene, showing that the interaction between fullerenes and the hydrogen-bonded foldamers is a general phenomenon.

Fluorescence experiments provided further evidence for the foldamer–fullerene interaction. Adding fullerenes to solutions of 1–5 in chloroform (containing 5% carbon disulfide, v/v) caused substantial reduction in the emission intensity of the folded molecules (Figure 2). Job plots revealed a 1:1 stoichiometry for C_{60} and foldamers 1–3 or the folded units in 4 and 5 (Figure 3).^[24] This observation suggests that the rigid aromatic amide linkers in bis-foldamer 4 and tris-foldamer 5 prevent the folded units from adopting a face-to-face arrangement and, consequently, inhibit the formation of sandwich-type complexes.^[19b] Once again, C_{70} was found to cause similar fluorescence quenching for each of the oligomers.

Association constants for 1–3 and apparent association constants^[25] for the folded units of 4 and 5 with C_{60} and C_{70} in chloroform were then evaluated using the fluorescence titration method.^[26] The values derived are listed in Table 1. Using the same method, data were also determined for the complexes of the $\text{MeO}\cdots\text{H}-\text{N}$ hydrogen-bonded foldamer 6. The values for 6 are significantly smaller than the corresponding values for 1, which may simply reflect the steric hindrance of the centrally located methyl groups in 6. Considering that all of the associations are just between two single aromatic units, the values in Table 1 are quite impressive. They are comparable with those of complexes formed

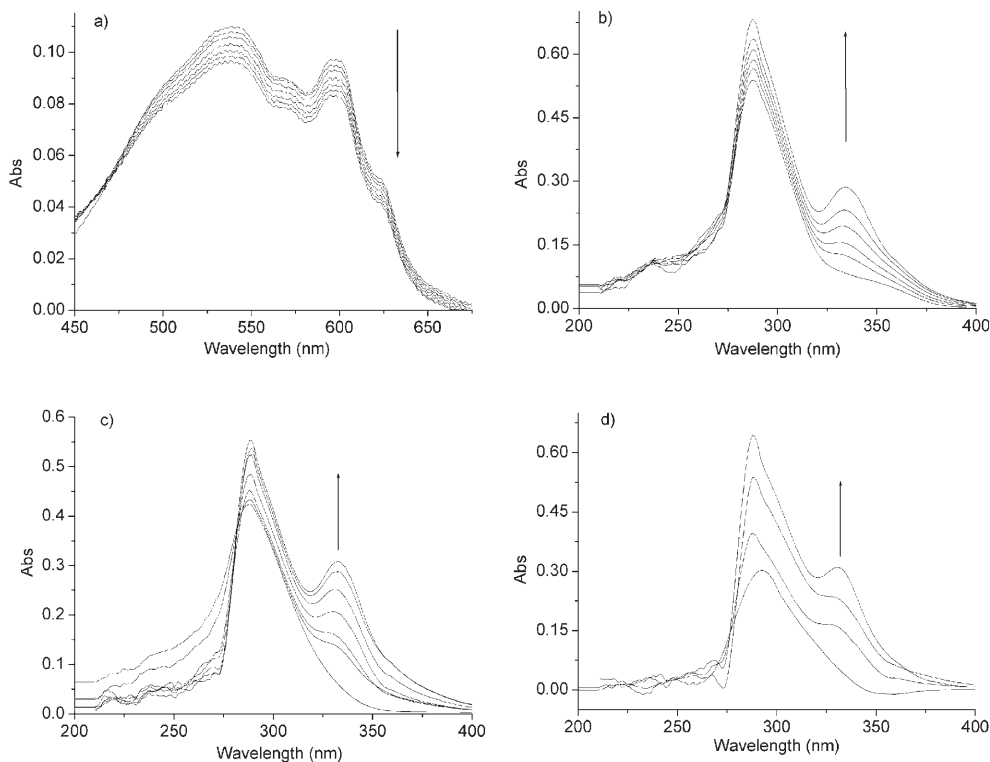


Figure 1. Changes in the absorption spectra of a) C_{60} (1.0×10^{-4} M) with the addition of **3** (0 to 1.1×10^{-4} M), b) **3** (9.0×10^{-6} M) with the addition of C_{60} (0 to 4.0×10^{-5} M), c) **4** (3.8×10^{-6} M) with the addition of C_{60} (0 to 1.6×10^{-5} M), and d) **5** (3.0×10^{-6} M) with the addition of C_{60} (0 to 1.5×10^{-5} M) in toluene at 25°C (the spectrum of the additive was subtracted from each of the spectra).

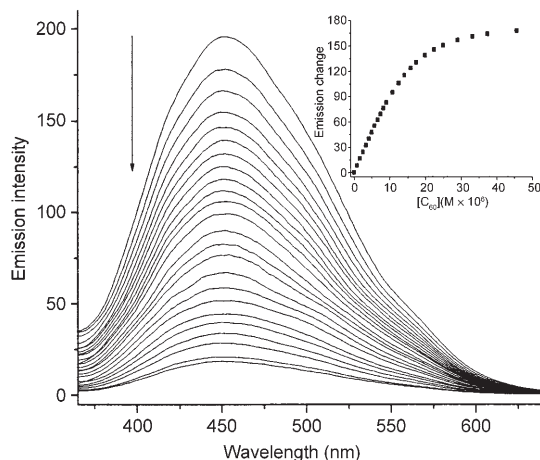


Figure 2. Fluorescence titration spectra of **4** (1.0×10^{-5} M) with the addition of C_{60} (0 to 4.6×10^{-5} M) in chloroform at 25°C (excitation wavelength = 328 nm).

between fullerenes and some bisporphyrin-based molecular tweezers.^[19b] CPK modeling revealed that the C–F bonds in the folded units of the oligomers form a slightly concave cyclic platform of diameter 9.0 Å.^[20b] The strong association between the F···H–N hydrogen-bonded foldamers and fullerenes may result from cooperative fluorophenyl···π interactions, as proposed by Row et al.,^[27,28] and solvophobic interactions (Figure 4). The fact that the values for C_{70} are consistently significantly larger than those for C_{60} implies

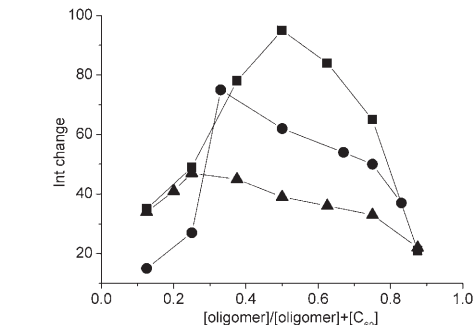


Figure 3. Job plots for complexes of C_{60} with **3** (■, $[\text{3}] + [\text{C}_{60}] = 1.6 \times 10^{-5}$ M, the emission change of **3** at 413 nm as probe), **4** (●, $[\text{4}] + [\text{C}_{60}] = 2.0 \times 10^{-5}$ M, the emission change of **4** at 458 nm as probe), and **5** (▲, $[\text{5}] + [\text{C}_{60}] = 1.0 \times 10^{-5}$ M, the emission change of **5** at 458 nm as probe) in chloroform at 25°C.

Table 1. (Apparent) association constants and associated free energies of the complexes between the foldamers or folded units and fullerenes in chloroform and carbon disulfide (19:1, v/v).^[a,b]

Complex	K_a [M ⁻¹]	ΔG [kJ mol ⁻¹]	Complex	K_a [M ⁻¹]	ΔG [kJ mol ⁻¹]
1 · C_{60}	1.4×10^4	-23.6	1 · C_{70}	2.6×10^4	-25.2
2 · C_{60}	3.0×10^4	-25.5	2 · C_{70}	3.8×10^4	-26.1
3 · C_{60}	1.8×10^4	-24.3	3 · C_{70}	2.3×10^4	-24.9
4 · C_{60} ^[c]	4.2×10^4	-26.4	4 · C_{70} ^[c]	5.3×10^4	-26.9
5 · C_{60} ^[c]	2.9×10^4	-25.4	5 · C_{70} ^[c]	3.3×10^4	-25.8
6 · C_{60}	2.8×10^3	-19.7	6 · C_{70}	3.8×10^3	-20.4

[a] The values are typically averages of two experiments performed at 25°C. [b] With an error of $\leq 15\%$. [c] Apparent association constant.

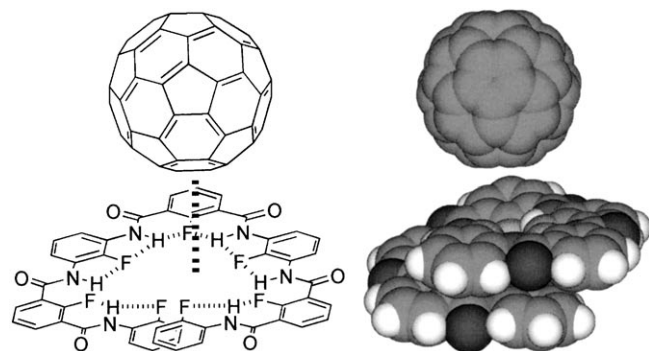


Figure 4. C–F... π interactions between the F–H–N hydrogen-bonded foldamers (with a heptamer as example) and C₆₀.

that its complexation with the foldamers mainly occurs at its extended equatorial region.^[11] The values for foldamer **3** are only slightly smaller than the corresponding values for bis-foldamer **4** and tris-foldamer **5**, indicating that there is no significant intramolecular cooperative effect for the folded units in **4** and **5**.

Adding C₆₀ to solutions of **1–3** in CDCl₃ and CS₂ (4:1, v/v) resulted in small but distinct changes in the signals in the downfield regions of their ¹H NMR spectra. Among the foldamers, **3** displayed the largest change upon mixing. The downfield regions of the spectra are shown in Figure 5 (for

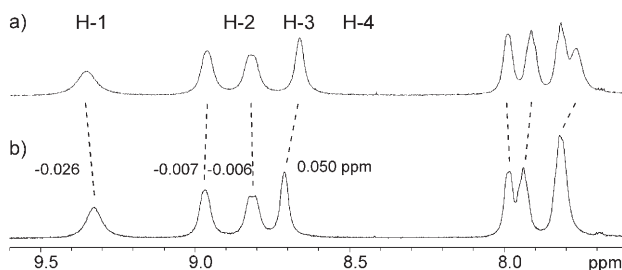


Figure 5. The downfield region of the ¹H NMR spectra of a) **3** (8.0 mM) and b) **3** + C₆₀ (1:1, 8.0 mM) in CDCl₃/CS₂ (4:1, v/v) at 25 °C.

the numbering, see the structure). The signals have been assigned on the basis of NOESY experiments. It can be seen that the change in shift for H-1 is distinctly larger than those for H-2 or H-3, while H-4 displays the largest change in shift.^[29] These observations suggest close proximity of the two species and that C₆₀ is favorably located to face the nitrated benzene ring. In the presence of 1 equiv of **3**, the ¹³C NMR signal of C₆₀ (8.0 mM) is shifted downfield by about 0.020 ppm. This small shift was consistently observed and, considering the spherical and rapidly rotating nature of C₆₀, may be taken as a further indication of its proximity to the folded structure.

The stacking properties and morphologies of **3–5** and their mixtures with C₆₀ were investigated by atomic force microscopy (AFM).^[30] All films were prepared by directly casting solutions (0.1 mM) in toluene on a mica plate and the AFM images were measured in tapping mode after

evaporation of the solvent. The images obtained from the residues of solutions of **3–5** are shown in Figure 6(a, c, d). Nano networks of fibrous assemblies may be discerned from the images of **3** and **4**, indicating efficient stacking of the folded units of both molecules in the solid state. Compared to those of **3**, the fibrils formed by **4** are obviously wider and thicker, which may be attributed to the formation of entangled assembled structures in the case of **4** due to its linear ditopic nature. In sharp contrast, discotic **5** only gave rise to separated particles of varying size (0.1 to 1 μ m). This result is very different from those observed for many C₃-symmetrical discotic derivatives that bear three planar aromatic moieties, which usually display a pronounced tendency to form fibrous aggregates.^[31]

For mixtures of the oligomers and C₆₀, the opposite stacking tendency was observed. Although a few linear fragmentary structures were generated, a 1:1 mixture of **3** and C₆₀ mainly gave rise to particles of <0.1 μ m in diameter (Figure 6b). This result indicates that the presence of C₆₀ efficiently breaks-up the fibrous assemblies of **3**, clearly by forming more stable **3**–C₆₀ stacking interactions. A mixture of **4** and C₆₀ produced more and longer fibrous structures, together with some small separated particles (Figure 6e). However, the fibrils were remarkably shorter and thinner than those observed for pure **4** (Figure 6c). Moreover, no networks were observed. Once again, these observations may be ascribed to the formation of strong stacking interactions between C₆₀ and the two folded units in **4**.

A mixture of **5** and C₆₀ generated unique honeycomb-like networks (Figure 6f). The width and thickness of the fibril bands were found to be approximately 30–150 and 5.5 nm, respectively (Figure 6h). Since in the cases of **3** and **4** the presence of C₆₀ substantially weakened the fibrous structures formed by the foldamers, this new network might be generated by continuous cooperative stacking interactions between the folded units of **5** and C₆₀, as shown in Figure 7. CPK modeling suggested a size of about 4.1 nm for the aromatic core of **5** (middle ring, Figure 8) and about 6.2 nm for the whole molecule of **5** (large ring, Figure 8). It is reasonable to assume that the size of the molecule in the packed state is smaller than the estimated value. Therefore, we propose that the fibrous networks formed by the mixture of **5** and C₆₀ are most likely produced by single-layer packing of the nano strands formed through continuous sandwich-like stacking of the upright or leaning tris-foldamer and C₆₀ on the surface, which is stabilized by intermolecular aggregation of the aliphatic chains (Figure 6).^[32]

Small-angle X-ray scattering (SAXS) experiments further supported the above packing pattern. The samples of pure **3–5** did not exhibit any major peaks (Figure 9a–c), implying that the folded units in these molecules are mainly randomly stacked in the solid state. In contrast, their mixtures with C₆₀ each produced a major peak, which corresponded to an ordered phase of size 2.9, 3.4, and 3.5 nm, respectively (Figure 9d–f). The strength of the peaks is substantially increased on going from **3** to **4** and **5**, suggesting a significant increase in the structural order. Moreover, the values for **4**

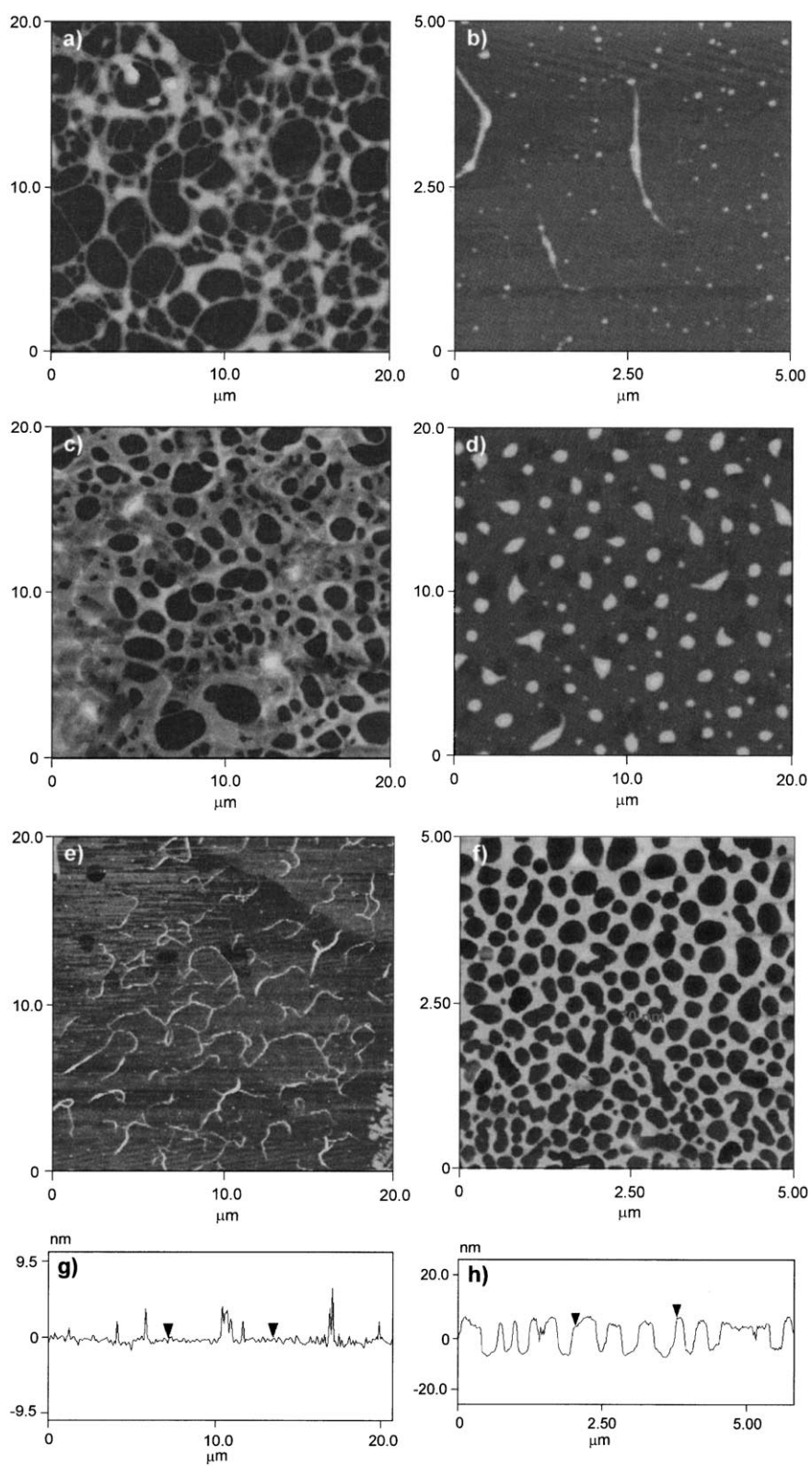


Figure 6. AFM images of drop-casts of solutions in toluene (0.1 mM) on a mica plate: a) **3**, b) **3** + C_{60} , c) **4**, d) **5**, e) **4** + C_{60} , and f) **5** + C_{60} ; g) typical height profile of the film in image e; h) typical height profile of the honeycomb-like fibrils in image f.

and **5** are very close to the sizes of their folded units (3.3 nm) (small ring, Figure 8). All of these observations

foldamers in the design of new materials. Considering the remarkable efficiency of this new stacking pattern, it should

support the view that ordered cylindrical aggregates are formed in the solid state through alternating stacking of the folded units and C_{60} molecules. Because such ordered aggregates are not exhibited by the pure samples, and the mixture of simple foldamer **3** and C_{60} exhibited only a weak peak, it is reasonable to propose that significant cooperation is involved in the stacking in the mixture of **5** and C_{60} , which leads to the most ordered cylindrical architecture. Similar cooperation should also occur for the mixture of **4** and C_{60} , albeit significantly more weakly. The lower intensity of the peaks observed for the mixture of **3** and C_{60} most likely reflects the reduced size of this foldamer.

Conclusions

We have demonstrated that strong interactions are formed between F···H–N hydrogen-bonded aromatic amide foldamers and fullerenes, both in solution and in the solid state. Quantitative fluorescence experiments have revealed that this unique interaction is considerably stronger than that in MeO···H–N hydrogen-bonded folded analogues. Cooperative C–F··· π and solvophobic interactions are proposed to explain the stacking. Although it is well known that large planar conjugated systems, such as porphyrins, have a propensity for π – π stacking with fullerenes, the present foldamer–fullerene interaction represents a unique new aromatic stacking pattern. The fact that fibrous nano networks have been assembled from a mixture of **5** and C_{60} illustrates the potential of the hydrogen-bonded

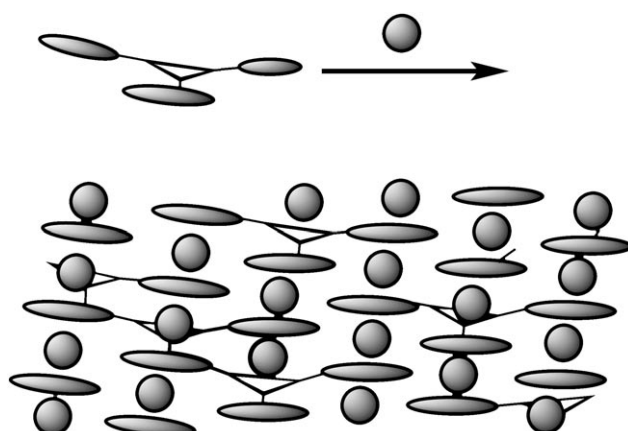


Figure 7. Proposed schematic diagram illustrating the packing behavior of the mixture of tris-foldamer **5** and C_{60} on the surface. The ellipsoids represent the folded units in **5** and the spheres represent C_{60} molecules.

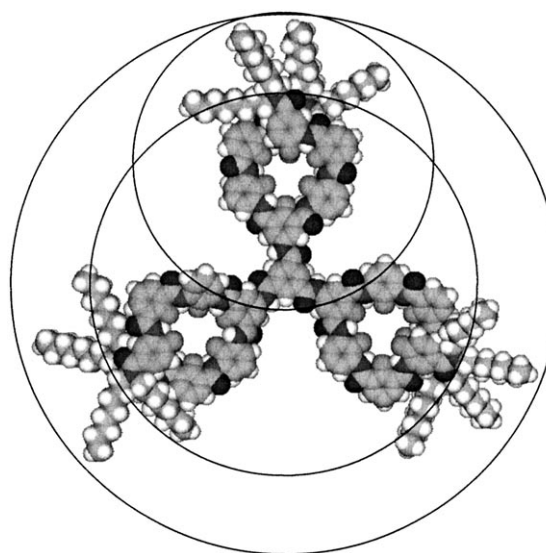


Figure 8. Extended CPK model of discotic tris-foldamer **5**. The sizes of the small, middle, and large rings are about 3.3, 4.1, and 6.2 nm, respectively.

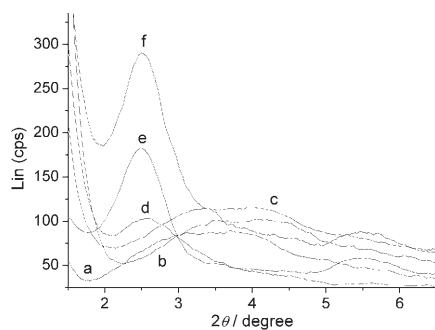


Figure 9. SAXS patterns of a) **3**, b) **4**, c) **5**, and of mixtures of C_{60} with d) **3** (molar ratio = 1:1), e) **4** (molar ratio = 2:1), and f) **5** (molar ratio = 3:1).

be possible to use the folded units as “jaws” in the development of a new type of molecular tweezers. Shape-persistent macrocycles may also be produced, which would be expected to exhibit interesting new properties.

Experimental Section

General methods: All reactions were carried out under a dry nitrogen atmosphere. Melting points are uncorrected. All solvents were dried before use following the standard procedures. Unless otherwise indicated, all starting materials were obtained from commercial suppliers and were used without further purification. Analytical thin-layer chromatography (TLC) was performed on glass plates coated with 0.2 mm of silica gel 60 with F_{254} indicator. ^1H NMR spectra were recorded on 300, 400 or 500 MHz spectrometers in the indicated solvents. Chemical shifts are expressed in parts per million (δ) using residual solvent protons as internal standards (^1H : chloroform: δ 7.26 ppm; DMSO: δ 2.49 ppm; ^{13}C : CDCl_3 : δ 77.23 ppm; ^{19}F : CFCl_3 : δ 0 ppm). Mass spectra (EI and MALDI-TOF) were obtained on a Varian Saturn 2000 or FTMS-7 spectrometer. Fluorescence spectra were recorded on an LS-50S fluorescence spectrometer. UV/Vis spectra were recorded on a Lambda 900 spectrophotometer. Elemental analysis was carried out at the SIOC analytical center.

Small-angle X-ray scattering (SAXS): SAXS measurements were made on a Bruker Nanostar system. Two-dimensional diffraction patterns were recorded using an image-intensified CCD detector. The experiments were carried out at room temperature (25°C) using $\text{Cu}_{\text{K}\alpha}$ radiation ($\lambda = 1.54 \text{ \AA}$) and operating at 40 kV and 35 mA.

Atomic force microscopy (AFM): AFM experiments were performed with a Nanoscope IIIa scanning probe microscope (Digital Instruments, Santa Barbara, CA). The tapping mode was employed in air using a tip fabricated from silicon (125 μm in length with a resonant frequency of ca. 500 kHz). Typical scan speeds during recording were 0.3–1 line s^{-1} and scan heads covered a maximum range of 20–20 μm . Samples were prepared by drop casting from solutions (10^{-5} M) in chloroform (containing 5 % CS_2) on freshly cleaved mica plates.

Typical procedures for fluorescence titrations and evaluation of the association constants K_a : Aliquots of a standard stock solution of the fullerene in chloroform were added to a solution of each foldamer receptor, and the mixtures were examined by fluorescence spectroscopy at 25°C . The spectra were corrected for the dilution factor. The difference (ΔI) in the emission intensities of the foldamers in the presence and absence of the fullerene was recorded and the data were plotted against [fullerene]. The association constants K_a for the 1:1 complexes were derived by means of nonlinear curve-fitting based on the equation:^[25b] $\Delta I = \Delta I_\infty - \frac{\infty((1+K_a[G]+K_a[H]_0) - ((1+K_a[G]+K_a[H]_0)^2 - 4K_a^2[H]_0[G])^{0.5})}{(2K_a[H]_0)}$, where $\Delta I = I - I_0$, $\Delta I_\infty = I_\infty - I_0$, $[G]$ is [fullerene], and $[H]_0$ = [foldamer]. For the 1:2 and 1:3 complexes of **4** and **5**, the apparent association constant K_a was evaluated from the same equation, but with $[H]_0 = 2 \times [4]$ or $3 \times [5]$.

Compound 8: At room temperature, diacid **7** (1.84 g, 10.0 mmol) was added to a stirred solution of concentrated nitric acid (65 %, 11 mL) and oleum (50 %, 12 mL). The mixture was stirred at 100°C for 6 h, cooled to room temperature, and then poured onto ice (100 g). The yellowish precipitate formed was collected by filtration, thoroughly washed with water, and dried. The crude product was purified by recrystallization from ethanol to give **8** as a pale yellow solid (1.15 g, 50 %). ^1H NMR ($[\text{D}_6]\text{DMSO}$): $\delta = 8.74 \text{ ppm}$ (*d*, $J = 5.7 \text{ Hz}$, 2 H); ^{13}C NMR ($[\text{D}_6]\text{DMSO}$): $\delta = 164.1$, 162.8, 142.9, 130.4, 122.3 ppm; ^{19}F NMR ($[\text{D}_6]\text{DMSO}$): $\delta = -99.1 \text{ ppm}$ (*t*, $J = 6.6 \text{ Hz}$, 1 F); MS (EI): m/z 229 [M^+]; elemental analysis calcd (%) for $\text{C}_8\text{H}_4\text{FNO}_6\text{H}_2\text{O}$: C 38.88, H 2.45, N 5.67; found: C 39.17, H 2.44, N 5.51.

Compound 3: Oxalyl chloride (0.50 g, 3.94 mmol) and DMF (10 mg) were added to a solution of **8** (92 mg, 0.40 mmol) in THF (20 mL). The solution was stirred at room temperature for 30 min and then concentrated under reduced pressure to give compound **9** as an oily solid. This

crude product was dissolved in THF (5 mL). The solution obtained was added dropwise to a solution of **10** (0.53 g, 0.80 mmol) and triethylamine (4.00 mL, 29.1 mmol) in THF (20 mL) and the mixture was stirred at room temperature for 2 h. After removal of the solvent under reduced pressure, the residue was redissolved in chloroform (40 mL). This solution was washed with dilute hydrochloric acid (1 N, 20 mL), saturated sodium hydrogen carbonate solution (20 mL), water (20 mL), and brine (20 mL), and then dried over sodium sulfate. After removal of the solvent in a rotary evaporator, the residue obtained was subjected to column chromatography (AcOEt/chloroform, 3:2, v/v) to give **3** as a pale yellow solid (0.47 g, 78%). ¹H NMR (CDCl_3): δ = 9.26 (d, J = 6.3 Hz, 2H), 8.95 (d, J = 8.1 Hz, 2H), 8.84–8.83 (m, 4H), 8.17 (d, J = 6.9 Hz, 2H), 8.03 (t, J = 6.9 Hz, 2H), 7.95–7.87 (m, 4H), 7.59 (d, J = 5.4 Hz, 2H), 7.26 (t, J = 5.4 Hz, 2H), 6.98–6.89 (m, 4H), 3.25 (t, J = 5.1 Hz, 4H), 3.11 (t, J = 5.1 Hz, 4H), 2.30 (s, 6H), 1.44–1.12 (m, 48H), 0.87–0.77 ppm (m, 12H); ¹³C NMR (CDCl_3): δ = 170.4, 161.2, 161.0, 159.5, 159.2, 158.6, 155.9, 154.7, 151.4, 144.7, 143.8, 141.5, 135.0, 134.8, 134.5, 134.4, 133.3, 133.2, 129.2–129.1 (m), 126.0, 125.8, 125.4, 125.3, 125.0–124.9 (m), 124.7, 124.5, 124.4, 123.3–123.2 (m), 122.8, 122.7, 122.6, 122.5, 121.0, 119.9, 119.8, 115.2, 114.9, 49.3, 45.2, 31.8, 31.7, 29.7, 29.3, 29.3, 29.0, 28.6, 27.3, 27.1, 26.5, 22.7, 22.6, 21.4, 14.1 ppm; ¹⁹F NMR (CDCl_3): δ = −105.0 (br, 1F), −115.1 (br, 2F), −126.8 (br, 2F), −145.6 ppm (br, 2F); MS (MALDI-TOF): m/z : 1526.7 [M+H]⁺; HRMS (MALDI-TOF): calcd for $\text{C}_{84}\text{H}_{100}\text{F}_7\text{N}_9\text{O}_{10}$: 1526.7349 [M]⁺; found: 1526.7363.

The following two compounds were prepared from the appropriate starting materials according to similar procedures.

Compound 4: ¹H NMR ([D₆]DMSO): δ = 10.86 (br, 2H), 10.38 (br, 4H), 10.36 (br, 4H), 10.32 (br, 4H), 8.68 (s, 1H), 8.38 (d, J = 5.7 Hz, 4H), 8.26 (d, J = 8.1 Hz, 2H), 7.95–7.83 (m, 12H), 7.79 (t, J = 7.2 Hz, 1H), 7.54–7.50 (m, 8H), 7.47 (t, J = 7.5 Hz, 4H), 7.38 (t, J = 9.6 Hz, 4H), 7.21–7.16 (m, 4H), 3.35 (br, 8H), 3.17 (br, 8H), 3.17 (s, 12H), 1.57–1.08 (m, 96H), 0.87–0.78 ppm (m, 24H); ¹³C NMR ([D₆]DMSO): δ = 169.2, 165.2, 165.1, 162.6–162.2 (m), 158.0, 155.8–155.6 (m), 154.6, 152.4, 134.6, 133.6, 133.5, 133.1, 133.0, 132.5–132.4 (m), 125.6–125.3 (m), 124.8–124.4 (m), 123.7–123.5 (m), 122.9–122.7 (m), 122.3–122.0 (m), 116.0, 115.7, 48.5, 44.4, 31.2, 29.0, 28.8–28.5 (m), 28.1–27.9 (m), 27.1–27.0 (m), 26.5–26.4 (m), 25.9–25.8 (m), 22.1, 20.7, 13.9 ppm; ¹⁹F NMR ([D₆]DMSO): δ = −115.4 (br, 4F), −120.4 (br, 2F), −122.0 to −122.2 (br, 4F), −136.1 to −136.3 ppm (br, 4F); MS (MALDI-TOF): m/z : 3145.1 [M+Na]⁺; HRMS (MALDI-TOF): calcd for $\text{C}_{176}\text{H}_{203}\text{F}_{14}\text{N}_{18}\text{O}_{18}$: 3122.5300 [M+H]⁺; found: 3122.5293.

Compound 5: ¹H NMR ([D₆]DMSO): δ = 11.01 (br, 3H), 10.37–10.31 (m, 18H), 8.85 (s, 3H), 8.37 (d, J = 5.7 Hz, 6H), 7.93 (t, J = 6.0 Hz, 6H), 7.87 (t, J = 7.2 Hz, 12H), 7.52–7.50 (m, 12H), 7.46 (t, J = 7.5 Hz, 6H), 7.37 (t, J = 9.6 Hz, 6H), 7.20–7.16 (m, 6H), 3.36 (br, 12H), 3.16 (br, 12H), 2.34 (s, 18H), 1.53–1.12 (m, 144H), 0.83–0.80 ppm (m, 36H); ¹³C NMR ([D₆]DMSO): δ = 174.3, 170.7, 169.7, 167.6–167.3 (m), 162.7, 160.6–160.5 (m), 159.4, 157.2, 140.3, 138.8, 138.7, 138.3, 138.2, 137.8–137.6 (m), 130.7–130.4 (m), 130.1–129.5 (m), 129.0–128.7 (m), 128.0–127.9 (m), 127.4–127.2 (m), 121.2, 120.9, 49.2, 36.4, 34.0, 34.2–33.5 (m), 33.3–33.1 (m), 32.4–32.1 (m), 31.7–31.5 (m), 31.2–31.0 (m), 27.3, 25.9, 19.1 ppm; ¹⁹F NMR ([D₆]DMSO): δ = −115.4 (s, 6F), −120.0 (s, 3F), −122.0 (d, J = 9.6 Hz, 6F), −136.1 ppm (t, J = 9.0 Hz, 6F); MS (MALDI-TOF): m/z : 4647.3 [M+H]⁺; elemental analysis calcd for $\text{C}_{261}\text{H}_{300}\text{F}_{21}\text{N}_{27}\text{O}_{27}\text{H}_2\text{O}$: C 67.20, H 6.54, N 8.11; found: C 66.92, H 6.55, N 7.90.

Compound 11: Pd/C (10%, 30 mg) was added to a solution of compound **3** (0.31 g, 0.20 mmol) in THF (40 mL). The suspension was stirred under 1 atmosphere of hydrogen gas at room temperature for 24 h. The solid was then filtered off and the solution was concentrated in a rotary evaporator. The residue obtained was purified by flash chromatography (AcOEt/chloroform, 3:2, v/v) to give **11** as a white solid (0.28 g, 95%). ¹H NMR (CDCl_3): δ = 9.02 (d, J = 10.5 Hz, 2H), 8.84 (d, J = 10.5 Hz, 2H), 8.67 (d, J = 10.5 Hz, 2H), 8.25 (d, J = 6.6 Hz, 2H), 8.08–8.01 (m, 4H), 7.81 (d, J = 5.1 Hz, 2H), 7.74 (d, J = 5.1 Hz, 2H), 7.33 (t, J = 7.8 Hz, 2H), 7.16 (d, J = 5.1 Hz, 2H), 6.98–6.95 (m, 4H), 4.126 (br, 2H), 3.37 (t, J = 5.1 Hz, 4H), 3.16 (t, J = 5.1 Hz, 4H), 2.25 (s, 6H), 1.51–1.14 (m, 48H), 0.87–0.78 ppm (m, 12H); ¹³C NMR (CDCl_3): δ = 170.3, 161.7, 161.1, 159.4, 156.0, 154.8, 151.5, 144.0, 140.8, 135.2, 135.1, 134.5, 134.4, 133.5, 125.9, 125.8, 125.5, 125.2, 125.0, 123.6, 123.5, 123.4, 122.8, 122.6, 121.2, 120.4,

119.0, 118.8, 115.3, 115.0, 49.3, 45.2, 31.8, 31.7, 30.3, 29.4, 29.3, 29.1, 28.6, 27.5, 27.1, 26.6, 22.7, 22.6, 21.5, 14.1 ppm; ¹⁹F NMR (CDCl_3): δ = −115.16 to −116.5 (br, 4F), −126.9 (br, 1F), −149.7 ppm (br, 2F); MS (MALDI-TOF): m/z : 1518.8 [M+Na]⁺; HRMS (MALDI-TOF): calcd for $\text{C}_{84}\text{H}_{100}\text{F}_7\text{N}_9\text{O}_{10}$: 1518.7393 [M+Na]⁺; found: 1518.7363.

Acknowledgements

We thank the National Natural Science Foundation (Nos. 20332040, 20425208, 20572126, 20621062, 20672137) and the National Basic Research Program of China (2007CB808000) for financial support.

- [1] a) F. Vögtle, *Supramolecular Chemistry*, Wiley, New York, **1991**, p. 285; b) J.-M. Lehn, *Supramolecular Chemistry, Concepts and Perspectives*, VCH, Weinheim, **1995**, p. 271; *Supramolecular Polymers* (Ed.: A. Ciferri), 2nd ed., CRC, Boca Raton, **2005**, p. 761.
- [2] a) L. Brunsved, B. J. B. Folmer, E. W. Meijer, R. P. Sijbesma, *Chem. Rev.* **2001**, *101*, 4071–4097; b) S. J. Rowan, S. J. Cantrill, G. R. L. Cousins, J. K. M. Sanders, J. F. Stoddart, *Angew. Chem.* **2002**, *114*, 938–993; *Angew. Chem. Int. Ed.* **2002**, *41*, 898–952; c) J.-M. Lehn, *Science* **2002**, *295*, 2400–2403; d) T. Shimizu, M. Masuda, H. Minamikawa, *Chem. Rev.* **2005**, *105*, 1401–1444; e) V. Percec, G. Ungar, M. Peterca, *Science* **2006**, *313*, 55–56; f) C. R. South, C. Burd, M. Weck, *Acc. Chem. Res.* **2007**, *40*, 63–74.
- [3] a) F. Zeng, S. C. Zimmerman, *Chem. Rev.* **1997**, *97*, 1681–1712; b) R. K. Castellano, D. M. Rudkevich, J. Rebek Jr., *Proc. Natl. Acad. Sci. USA* **1997**, *94*, 7132–7137; c) M. J. Krische, J.-M. Lehn, *Struct. Bonding (Berlin)* **2000**, *96*, 3–29; d) R. Shenhav, V. M. Rotello, *Acc. Chem. Res.* **2003**, *36*, 549–561; e) A. Ajayaghosh, S. J. George, A. P. H. J. Schenning, *Top. Curr. Chem.* **2005**, *258*, 83–118; f) F. Huang, H. W. Gibson, *Prog. Polym. Sci.* **2005**, *30*, 982–1018.
- [4] a) S. Leininger, B. Olenyuk, P. J. Stang, *Chem. Rev.* **2000**, *100*, 853–908; b) B. J. Holliday, C. A. Mirkin, *Angew. Chem.* **2001**, *113*, 2076–2097; *Angew. Chem. Int. Ed.* **2001**, *40*, 2022–2043; c) U. S. Schubert, C. Eschbaumer, *Angew. Chem.* **2002**, *114*, 3016–3050; *Angew. Chem. Int. Ed.* **2002**, *41*, 2892–2926; d) C.-C. You, R. Dobrawa, C. R. Saha-Möller, F. Würthner, *Top. Curr. Chem.* **2005**, *258*, 39–82.
- [5] a) M. L. Bushey, T.-Q. Nguyen, W. Zhang, D. Horoszewski, C. Nuckolls, *Angew. Chem.* **2004**, *116*, 5562–5570; *Angew. Chem. Int. Ed.* **2004**, *43*, 5446–5453; b) A. P. H. J. Schenning, E. W. Meijer, *Chem. Commun.* **2005**, 3245–3258; c) K. Araki, I. Yoshikawa, *Top. Curr. Chem.* **2005**, *256*, 133–165.
- [6] a) *Fullerenes: Chemistry, Physics, and Technology* (Eds.: K. M. Kadish, R. S. Ruoff), Wiley, New York, **2000**, p. 968; b) *Fullerenes: From Synthesis to Optoelectronic Properties* (Eds.: D. M. Guldi, N. Martin), Kluwer, Dordrecht, **2002**, p. 440; c) *Fullerenes: Chemistry and Reactions* (Eds.: A. Hirsch, M. Brettelrich), Wiley-VCH, Weinheim, **2005**, p. 423.
- [7] a) A. Hirsch, *Adv. Mater.* **1993**, *5*, 859–861; b) M. Prato, *Top. Curr. Chem.* **1999**, *199*, 173–187; c) J.-F. Nierengarten, *Top. Curr. Chem.* **2003**, *228*, 87–110; d) J. Roncali, *Chem. Soc. Rev.* **2005**, *34*, 483–495; e) D. M. Guldi, F. Zerbetto, V. Georgakilas, M. Prato, *Acc. Chem. Res.* **2005**, *38*, 38–43.
- [8] a) L. Dai, A. W. H. Mau, *Adv. Mater.* **2001**, *13*, 89–913; b) M. E. Mackay, A. Tuteja, P. M. Duxbury, C. J. Hawker, B. Van Horn, Z. Guan, G. Chen, R. S. Krishnan, *Science* **2006**, *311*, 1740–1743.
- [9] a) M. Shirakawa, N. Fujita, S. Shinkai, *J. Am. Chem. Soc.* **2003**, *125*, 9902–9903; b) Y. Liu, H. Wang, P. Liang, H.-Y. Zhang, *Angew. Chem.* **2004**, *116*, 2744–2748; *Angew. Chem. Int. Ed.* **2004**, *43*, 2690–2694; c) M. Wolfs, F. J. M. Hoeben, E. H. A. Beckers, A. P. H. J. Schenning, E. W. Meijer, *J. Am. Chem. Soc.* **2005**, *127*, 13484–13485; d) G. D. Panto, J.-L. Wietor, J. K. M. Sanders, *Angew. Chem.* **2007**, *119*, 2288–2290; *Angew. Chem. Int. Ed.* **2007**, *46*, 2238–2240.
- [10] a) F. Diederich, M. Gómez-López, *Chem. Soc. Rev.* **1999**, *28*, 263–277; b) T. Haino, M. Yanase, Y. Fukazawa, *Angew. Chem.* **1998**, *110*,

- 1044–1046; *Angew. Chem. Int. Ed.* **1998**, *37*, 997–999; c) A. Ikeda, M. Yoshimura, H. Udzu, C. Fukuhara, S. Shinkai, *J. Am. Chem. Soc.* **1999**, *121*, 4296–4297; d) J. L. Atwood, L. J. Barbour, M. W. Heaven, C. L. Raston, *Angew. Chem.* **2003**, *115*, 3376–3379; *Angew. Chem. Int. Ed.* **2003**, *42*, 3254–3257; e) M.-X. Wang, X.-H. Zhang, Q.-Y. Zheng, *Angew. Chem.* **2004**, *116*, 856–860; *Angew. Chem. Int. Ed.* **2004**, *43*, 838–842; f) E. M. Pérez, M. Sierra, L. Sánchez, M. R. Torres, R. Viruela, P. M. Viruela, E. Ortí, N. Martín, *Angew. Chem.* **2007**, *119*, 1879–1883; *Angew. Chem. Int. Ed.* **2007**, *46*, 1847–1851.
- [11] a) T. Konishi, A. Ikeda, S. Shinkai, *Tetrahedron* **2005**, *61*, 4881–4899; b) P. D. W. Boyd, C. A. Reed, *Acc. Chem. Res.* **2005**, *38*, 235–242; c) K. Tashiro, T. Aida, *Chem. Soc. Rev.* **2007**, *36*, 189–197.
- [12] G.-B. Pan, X.-H. Cheng, S. Höger, W. Freyland, *J. Am. Chem. Soc.* **2006**, *128*, 4218–4219.
- [13] E. M. Pérez, L. Sánchez, G. Fernández, N. Martín, *J. Am. Chem. Soc.* **2006**, *128*, 7172–7173.
- [14] a) D. Seebach, J. L. Mathews, *Chem. Commun.* **1997**, 2015–2022; b) S. H. Gellman, *Acc. Chem. Res.* **1998**, *31*, 173–180; c) K. D. Stiglers, M. J. Soth, J. S. Nowick, *Curr. Opin. Chem. Biol.* **1999**, *3*, 714–723; d) D. J. Hill, M. J. Mio, R. B. Prince, T. S. Hughes, J. S. Moore, *Chem. Rev.* **2001**, *101*, 3893–4011; e) M. S. Cubberley, B. L. Iverson, *Curr. Opin. Chem. Biol.* **2001**, *5*, 650–653; f) C. Schmuck, *Angew. Chem.* **2003**, *115*, 2552–2556; *Angew. Chem. Int. Ed.* **2003**, *42*, 2448–2452; g) R. P. Cheng, *Curr. Opin. Struct. Biol.* **2004**, *14*, 512–520; h) G. Licini, L. J. Prins, P. Scrimin, *Eur. J. Org. Chem.* **2005**, 969–977; i) X. Li, D. Yang, *Chem. Commun.* **2006**, 3367–3379; j) M. T. Stone, J. M. Heemstra, J. S. Moore, *Acc. Chem. Res.* **2006**, *39*, 11–20.
- [15] a) B. Gong, *Chem. Eur. J.* **2001**, *7*, 4336–4342; b) A. R. Sanford, B. Gong, *Curr. Org. Chem.* **2003**, *7*, 1649–1650; c) I. Huc, *Eur. J. Org. Chem.* **2004**, 17–29; d) Z.-T. Li, J.-L. Hou, C. Li, H.-P. Yi, *Chem. Asian J.* **2006**, *1*, 766–778.
- [16] Y. Hamuro, S. J. Geib, A. D. Hamilton, *J. Am. Chem. Soc.* **1996**, *118*, 7529–7541.
- [17] For recent representative examples, see: a) L. H. Yuan, H. Q. Zeng, K. Yamato, A. R. Sanford, W. Feng, H. Atreya, D. K. Sukumaran, T. Szyperski, B. Gong, *J. Am. Chem. Soc.* **2004**, *126*, 16528–16537; b) C. Dolain, J.-M. Léger, N. Delsuc, H. Gornitzka, I. Huc, *Proc. Natl. Acad. Sci. USA* **2005**, *102*, 16146–16151; c) E. Kolomietz, V. Berl, I. Odriozola, A.-M. Stadler, N. Kyritsakas, J.-M. Lehn, *Chem. Commun.* **2003**, 2868–2869; d) D. Kanamori, T. Okamura, H. Yamamoto, N. Ueyama, *Angew. Chem.* **2005**, *117*, 995–998; *Angew. Chem. Int. Ed.* **2005**, *44*, 969–972; e) M. F. Mayer, S. Nakashima, S. C. Zimmerman, *Org. Lett.* **2005**, *7*, 3005–3008; f) H. Masu, M. Sakai, K. Kishikawa, M. Yamamoto, K. Yamaguchi, S. Kohmoto, *J. Org. Chem.* **2005**, *70*, 1423–1431; g) R. W. Sinkeldam, M. H. C. J. van Houtem, G. Koeckelberghs, J. A. J. M. Vekemans, E. W. Meijer, *Org. Lett.* **2006**, *8*, 383–386.
- [18] a) J. Zhu, X.-Z. Wang, Y.-Q. Chen, X.-K. Jiang, X.-Z. Chen, Z.-T. Li, *J. Org. Chem.* **2004**, *69*, 6221–6227; b) J. Zhu, J.-B. Lin, Y.-X. Xu, X.-B. Shao, X.-K. Jiang, Z.-T. Li, *J. Am. Chem. Soc.* **2006**, *128*, 12307–12313; c) J. Zhu, J.-B. Lin, Y.-X. Xu, X.-K. Jiang, Z.-T. Li, *Tetrahedron* **2006**, *62*, 11933–11941.
- [19] a) J.-L. Hou, X.-B. Shao, G.-J. Chen, Y.-X. Zhou, X.-K. Jiang, Z.-T. Li, *J. Am. Chem. Soc.* **2004**, *126*, 12386–12394; b) Z.-Q. Wu, X.-B. Shao, C. Li, J.-L. Hou, K. Wang, X.-K. Jiang, Z.-T. Li, *J. Am. Chem. Soc.* **2005**, *127*, 17460–17468; c) J.-L. Hou, H.-P. Yi, X.-B. Shao, C. Li, Z.-Q. Wu, X.-K. Jiang, L.-Z. Wu, C.-H. Tung, Z.-T. Li, *Angew. Chem.* **2006**, *118*, 810–815; *Angew. Chem. Int. Ed.* **2006**, *45*, 796–800; d) H.-P. Yi, J. Wu, K.-L. Ding, X.-K. Jiang, Z.-T. Li, *J. Org. Chem.* **2007**, *72*, 870.
- [20] a) X. Zhao, X.-Z. Wang, X.-K. Jiang, Y.-Q. Chen, Z.-T. Li, G.-J. Chen, *J. Am. Chem. Soc.* **2003**, *125*, 15128–15139; b) C. Li, S.-F. Ren, J.-L. Hou, H.-P. Yi, S.-Z. Zhu, X.-K. Jiang, Z.-T. Li, *Angew. Chem.* **2005**, *117*, 5871–5875; *Angew. Chem. Int. Ed.* **2005**, *44*, 5725–5729; c) Y.-Y. Zhu, J. Wu, C. Li, J. Zhu, J.-L. Hou, C.-Z. Li, X.-K. Jiang, Z.-T. Li, *Cryst. Growth Des.* **2007**, *8*, 1490–1496.
- [21] H.-P. Yi, C. Li, J.-L. Hou, X.-J. Jiang, Z.-T. Li, *Tetrahedron* **2005**, *61*, 7974–7980.
- [22] Folded hydrogen-bonded dendrimers have been reported: a) J. W. Lockman, N. M. Paul, J. R. Parquette, *Prog. Polym. Sci.* **2005**, *30*, 423–452; b) H. Shao, J. W. Lockman, J. R. Parquette, *J. Am. Chem. Soc.* **2007**, *129*, 1884–1885.
- [23] K. Reichenbächer, H. I. Süss, J. Hulliger, *Chem. Soc. Rev.* **2005**, *34*, 22–30.
- [24] P. Job, *Ann. Chim. Ser. 10*, **1928**, *9*, 113–203.
- [25] The association constant may be regarded as the average value of K_a of the foldamer units in **4** and **5**. For recent examples, see ref. [19b,c] and also: a) T. Hasobe, H. Imahori, P. C. Kamat, T. K. Ahn, S. K. Kim, D. Kim, A. Fujimoto, T. Hirakawa, S. Fukuzumi, *J. Am. Chem. Soc.* **2005**, *127*, 1216–1228; b) W.-S. Li, D.-L. Jiang, Y. Suna, T. Aida, *J. Am. Chem. Soc.* **2005**, *127*, 7700–7702.
- [26] K. A. Conners, *Binding Constants: The Measurement of Molecular Complex Stability*, Wiley, New York, **1987**.
- [27] a) M. D. Prasanna, T. N. G. Row, *Cryst. Eng.* **2000**, *3*, 135–154; b) F. Babudri, G. M. Farinola, F. Naso, R. Ragni, *Chem. Commun.* **2007**, 1003–1022.
- [28] Phenyl-perfluorophenyl interactions have been reported: a) G. W. Coates, A. R. Dunn, L. M. Henling, J. W. Ziller, E. B. Lobkovsky, R. H. Grubbs, *J. Am. Chem. Soc.* **1998**, *120*, 3641–3649; b) F. Ponzianni, R. Zagha, K. Hardcastle, J. S. Siegel, *Angew. Chem.* **2000**, *112*, 2413–2415; *Angew. Chem. Int. Ed.* **2000**, *39*, 2323–2325; c) M. Gdaniec, W. Jankowski, M. J. Milewska, T. Polonski, *Angew. Chem.* **2003**, *115*, 4033–4036; *Angew. Chem. Int. Ed.* **2003**, *42*, 3903–3906; d) S. W. Watt, C. Dai, A. J. Scott, J. M. Burke, R. L. Thomas, J. C. Collings, C. Viney, W. Clegg, T. B. Marder, *Angew. Chem.* **2004**, *116*, 3123–3125; *Angew. Chem. Int. Ed.* **2004**, *43*, 3061–3063; e) L. Shu, M. Mayor, *Chem. Commun.* **2006**, 4134–4136.
- [29] The result is consistent with reported observations that fullerenes usually cause small or imperceptible shifts in the signals of cyclophane receptors in their ^1H NMR spectra, see ref. [10e,f] and also: H.-Y. Gong, X.-H. Zhang, D.-X. Wang, H.-W. Ma, Q.-Y. Zheng, M.-X. Wang, *Chem. Eur. J.* **2006**, *12*, 9262.
- [30] Examples of foldamer stacking have been reported, see: a) M. S. Cubberley, B. L. Iverson, *J. Am. Chem. Soc.* **2001**, *123*, 7560–7563; b) C. Kübel, M. J. Mio, J. S. Moore, D. C. Martin, *J. Am. Chem. Soc.* **2002**, *124*, 8605–8610; c) J. J. Han, W. Wang, A. D. Q. Li, *J. Am. Chem. Soc.* **2006**, *128*, 672–673; d) R. W. Sinkeldam, F. J. M. Hoeben, M. J. Pouderoijen, I. De Cat, J. Zhang, S. Furukawa, S. De Feyter, J. A. J. M. Vekemans, E. W. Meijer, *J. Am. Chem. Soc.* **2006**, *128*, 16113–16121.
- [31] For representative examples of the aggregation of C_3 -symmetrical discotic molecules, see: a) A. R. A. Palmans, J. A. J. M. Vekemans, E. E. Havinga, E. W. Meijer, *Angew. Chem.* **1997**, *109*, 2763–2765; *Angew. Chem. Int. Ed. Engl.* **1997**, *36*, 2648–2651; b) M. L. Bushey, T.-Q. Nguyen, W. Zhang, D. Horoszewski, C. Nuckolls, *Angew. Chem.* **2004**, *116*, 5562–5570; *Angew. Chem. Int. Ed.* **2004**, *43*, 5546–5549; c) A. Sakamoto, D. Ogata, T. Shikata, K. Hanabusa, *Macromolecules* **2005**, *38*, 8983–8986; d) J. J. Van Gorp, J. A. J. M. Vekemans, E. W. Meijer, *J. Am. Chem. Soc.* **2002**, *124*, 14759–14769; e) M. Blomenhofer, S. Ganzleben, D. Hanft, H.-W. Schmidt, M. Kristiansen, P. Smith, K. Stoll, D. Mader, K. Hoffmann, *Macromolecules* **2005**, *38*, 3688–3695; f) J. van Herrikhuyzen, P. Jonkheijm, A. P. H. J. Schenning, E. W. Meijer, *Org. Biomol. Chem.* **2006**, *4*, 1539–1545.
- [32] Other kinds of entangled or cross-stacked assembling motifs are not excluded. However, the proposed packing motif could explain the thickness of the fibrous bands in Figure 6h.

Received: July 7, 2007
Published online: September 21, 2007